This article has been accepted for publication in a future issue of this journal, but has not been fully edited. Content may change prior to final publication. Citation information: DOI 10.1109/TAP.2014.2350520, IEEE Transactions on Antennas and Propagation

300-GHz Step-profiled Corrugated Horn Antennas Integrated in LTCC

Takuro Tajima, Ho-Jin Song, Katsuhiro Ajito, *Member, IEEE,* Makoto Yaita, *non Member, IEEE,* and Naoya Kukutsu *Member, IEEE*

***Abstract*—This paper presents 300-GHz step-profiled corrugated horn antennas, aiming at their integration in low-temperature co-fired ceramic (LTCC) packages. Using substrate integrated waveguide technology, the cavity inside the multi-layer LTCC substrate and a surrounding via fence are used to form a feeding hollow waveguide and horn structure. Owing to the vertical configuration, we were able to design the corrugations and stepped profile of horn antennas to approximate smooth metallic surface. To verify the design experimentally, the LTCC waveguides and horn antennas were fabricated with an LTCC multi-layer process. The LTCC waveguide exhibits insertion loss of 0.6 dB/mm, and the LTCC horn antenna exhibits 18-dBi peak gain and 100-GHz bandwidth with more than 10-dB return loss. The size of the horn antenna is only 5×5×2.8mm^3, which makes it easy to integrate it in LTCC transceiver modules.**

***Index Terms*—low-temperature co-fired ceramics (LTCC), dielectric substrates, horn antennas, terahertz (THz)**

I. Introduction

With the recent spread of 4K televisions and hi-vision video cameras in the consumer market, the demand for massive data transfer will push data rates higher in broadband wireless communications. Data rates of mobile phones will also become higher year by year, reaching tens of gigabits in a few decades. Terahertz (THz) communications is one of the promising ways to realize such high-speed data transfer [1, 2]. Although the THz bands have a limitation on transmission range due to high atmospheric attenuation, their wide bandwidth allows us to attain high data rates even with a simple modulation scheme, such as amplitude shift keying [3].

Many THz packages have been made of metal, and a silicon lens has been employed as an integrated antenna. However, reduction of their cost and size will open up various applications. For millimeter-wave packages, low-temperature co-fired ceramic (LTCC) has become one of the standard materials because of high-integration capability and low cost for high-volume production. Planar antennas, passive components and a monolithic microwave integrated circuit (MMIC) have already been integrated in an LTCC multi-layer package based on antenna-in-package (AIP) technology [4]. In THz bands, the further scaling of antennas enables various antennas to be integrated inside a radio package. Being compatible with system-in-package technology, LTCC also shows potential for use in sub-millimeter or even THz wireless transceiver modules.

The LTCC multi-layer and via process enables us to form a three-dimensional antenna structure to achieve desirable radiation characteristics. Sub-millimeter-wave integrated antennas, such as 140-GHz and 270-GHz slot array antennas, 270-GHz lens antenna, and 140-GHz SIW *H*-plane horn antennas, based on substrate integrated waveguide (SIW) technology have been reported [5]–[9]. For frequencies above a few hundred gigahertz, manufacturing errors become crucial with respect to antenna characteristics, so a simple structure, such as horn, is preferred. To take advantage the THz band, antennas must have wide bandwidth and high gain. A horn antenna exhibits inherent wideband and moderate gain. Antenna gain of a horn antenna is described as $G \sim L/\lambda_0$, where L is horn length and λ_0 is free-space wavelength. As the free-space wavelength is around 1.0 mm in the 300-GHz band, 10-dBi gain can be achievable even for horn length of a few millimeters. Furthermore, the size of a standard waveguide is scaled down to below 1 mm^2, so that horn antennas based on SIW technology are suitable for compact packaging.

In a conventional SIW horn antenna, dielectric layers are formed parallel to the *H* plane, so that the SIW horn antenna is filled with dielectric. One of the main problems with SIW horn antennas is the mismatch between the edge of the dielectric slab and air, which decreases the operational bandwidth [10]. Thus, a metallic grating structure at the horn aperture has been employed [11]. The dielectric loss and conductor loss also become problematic in the THz band, which degrades antenna efficiency. To obtain better efficiency, a hollow SIW slot array antenna in the 60-GHz band was proposed [12]. In our previous study, a vertical hollow SIW horn with the LTCC multi-layer process was proposed to tackle these issues [13]. The preliminary results showed that gain and bandwidth are limited by the fabrication variation in flare formation and that the corrugation of inner wall affects the center frequency of the operational band.

In this paper, we numerically and experimentally investigate hollow corrugated waveguides and step-profiled corrugated horn antennas in the 300-GHz band to improve gain and bandwidth. This paper is organized as follows. In section II, we describe the basic concept of the design, which are hollow waveguide and horn vertically formed inside multiple stacked LTCC layers. To verify this concept, an LTCC hollow

Manuscript received December 2, 2013; revised May 8, 2014.This work was supported in part by the research and development program "Multi-ten Gigabit Wireless Communications Technology at Sub-terahertz Frequencies" of the Ministry of Internal Affairs and Communications, Japan.

The Authors are with the NTT Device Technology Laboratories, NTT Corporation, Kanagawa 243-0198, Japan (tajima.takurou@lab.ntt.co.jp).

This article has been accepted for publication in a future issue of this journal, but has not been fully edited. Content may change prior to final publication. Citation information: DOI 10.1109/TAP.2014.2350520, IEEE Transactions on Antennas and Propagation

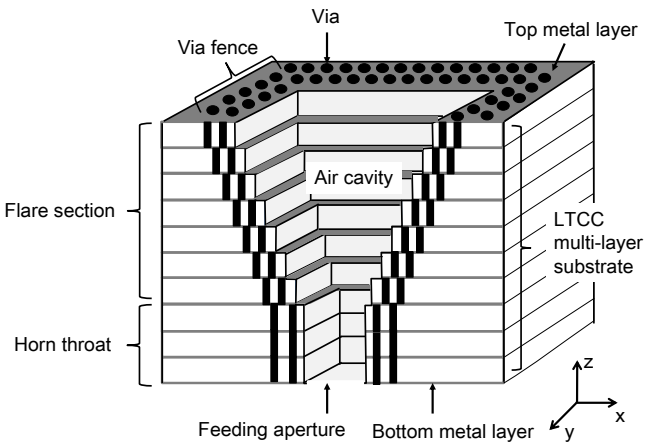

Fig. 1. Concept of the proposed LTCC horn antenna.

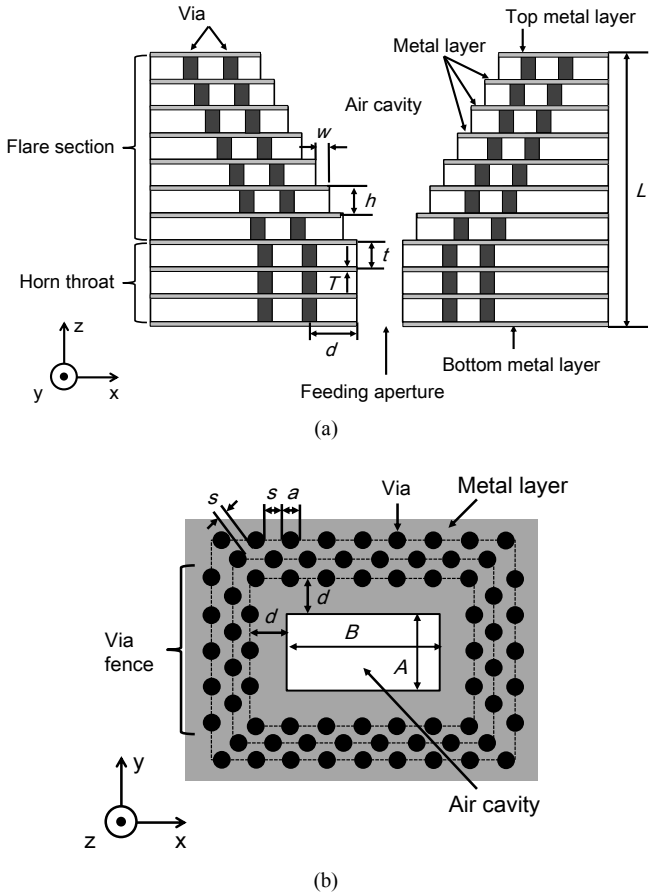

Fig. 2. Configuration of the proposed horn antenna integrated in LTCC. (a) Cross-sectional view of the LTCC horn antenna; (b) top view of the LTCC hollow waveguide.

corrugated waveguide was numerically analyzed, fabricated, and measured. Then we applied the vertical hollow structure to a step-profile horn antenna. The design of horn antenna is parametrically studied and its design factors for improving the antenna characteristics are discussed. In section III, we present a fabricated prototype of the LTCC horn antenna and show measured return loss, antenna gain, and the radiation pattern, which confirm the simulations.

TABLE I
DESIGN RULES OF LTCC MULTI-LAYER PROCESS

Symbol	Parameters	Value
a	Via diameter	100 μm
s	Via spacing	100 μm
t	Layer thickness	100 μm
T	Metal thickness	5 μm
L	Total thickness	< 3000 μm
d	Via distance from cavity edge	> 150 μm
ϵ_r	Dielectric constant of LTCC	6.7
δ	Loss tangent of LTCC	0.02
ρ	Conductivity of silver	3.3×10^7 S/m

II. DESIGN

A. Antenna Structure

Fig. 1 illustrates the concept of a horn antenna integrated on an LTCC multi-layer substrate. A step-profiled SIW horn antenna is designed using multi-layer substrates to approximate the radiation characteristics of smooth-wall pyramidal horn antenna. The proposed SIW horn antenna doesn't have impedance mismatch at the horn aperture thanks to its hollow structure. Furthermore this vertical configuration offers flexibility in controlling the aperture design compared to a conventional *H*-plane SIW horn antenna, which results in better antenna gain and *E*/*H* symmetry of the radiation patterns.

A rectangular horn structure is formed in the air cavity of the LTCC multi-layer substrate surrounded by metal layers and a via fence as shown in Fig. 2 (a). The vias are filled with silver paste in each layer and located at a uniform distance from the edge of the cavity in each layer. A metal pattern of silver is printed on the upper side of the LTCC sheet to provide electrical connection between the vias. To form the hollow structure at the horn throat, a rectangular cavity (A = 0.4 mm, B = 0.8 mm) is formed by the layers with the same cavity size and surrounded by the via fences. The layer-to-layer alignment in LTCC process is less than 50 μm. Consequently, to shape the flare of the horn, gradually widening cavities are drilled into each LTCC sheet. Thus, the horn antenna inherently has a stepped profile as shown in Fig. 2(a). In this study, step sizes are uniform along the flare of horn. The metal layers cover the top of each step by the edge of cavity. One issue in using LTCC as a substrate for sub-millimeter applications is its loss tangent. From a frequency-domain spectroscopic analysis, we estimated the dielectric constant and loss tangent of LTCC in the 300-GHz band to be 6.7 and 0.02, respectively. Notably, the loss tangent is twice that for 60 GHz [12]. To resolve this issue, the hollow SIW effectively reduces the dielectric loss of LTCC and enhances antenna efficiency. As we configure the SIW vertically in the stacked LTCC layers, it can be fabricated without any special process.

Another issue is the leakage of electro-magnetic waves through the metallic mesh structure. In order to prevent leakage of electromagnetic waves between vias and metal layers, the via spacing and thickness of the LTCC layers should be smaller than a quarter wavelength. The wavelength in LTCC is $\lambda_s = \lambda_0/\sqrt{\epsilon_r}$ = 0.39 mm at 300 GHz, so that we set a and s to

This article has been accepted for publication in a future issue of this journal, but has not been fully edited. Content may change prior to final publication. Citation information: DOI 10.1109/TAP.2014.2350520, IEEE Transactions on Antennas and Propagation

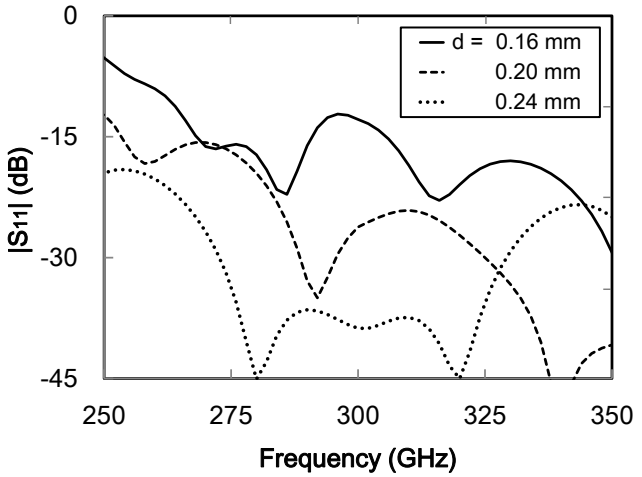

Fig. 3. Simulated $|S_{11}|$ of the LTCC hollow waveguide for different slot depths.

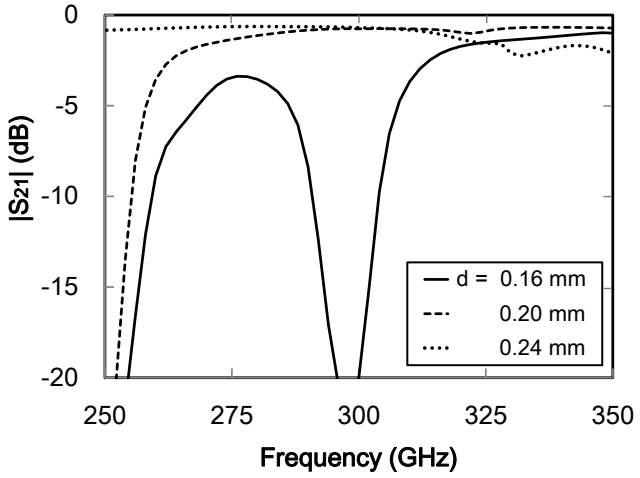

Fig. 4. Simulated $|S_{21}|$ of the LTCC hollow waveguide for different slot depths.

the minimum value in the manufacture design rule: $a = 0.1$ mm; $s = 0.1$ mm. Moreover, three rows of via fences are used to reduce the leakage as shown in Fig. 2(b). Design rules of the LTCC multi-layer process are depicted in Table I.

B. Vertical Substrate Integrated Waveguide

The substrate integrated waveguide is vertically formed through the layers by drilling cavities and vias. Since the thin LTCC sheets can be easily torn during the via drilling process, some space is required between the via fence and the cavity region. For this purpose, the inner wall of the hollow waveguide is covered with a few hundred micrometers of a dielectric. The distance between the edge of the cavity and the center of the via fence is denoted as d in Fig. 2 (b). In 300-GHz band, d becomes comparable to the wavelength, so that the inner wall cannot approximate a simple metallic wall. To reduce electromagnetic waves travelling into the dielectric, we covered this region on each layer with a metal layer. As a result, dielectric-loaded slots uniformly exist on the four inner walls of the SIW. Thus, the waveguide is considered to have a structure equivalent to that of a conventional corrugated waveguide.

A corrugated waveguide is known as a low-loss waveguide because of the reduction of wall current. Corrugated waveguides are commonly designed to convert the TE_{10} mode into the HE_{10} mode, and slot depth is designed to be a capacitive surface, i.e. a quarter wavelength. When surface impedance is capacitive, the tangential magnetic field vanishes at the wall. The transmission characteristics of a rectangular corrugated waveguide have been analytically and numerically studied in the literature [14]–[17]. As slots on the inner walls consist of LTCC layers sandwiched by thin metal layers, metal thickness T and the thickness of the LTCC layers t correspond to the thickness of the corrugation teeth and the slot width, respectively. In this corrugation, T is small compared to the free-space wavelength λ_0 and slot depth. Under the above assumptions, the propagation constant is determined by slot width t, pitch $t + T$, and effective slot depth d_{eff}. For the thickness of the corrugation teeth that are sufficiently thin, $T < t/10$, the approximate surface reactance is given by [18]

$$\mathrm{X} = \frac{t}{t+T}\sqrt{\frac{\mu_s}{\epsilon_s}}\tan\left(k_s d_{eff}\right) \quad (1)$$

Where μ_s is the permeability of LTCC and k_s is the wave number. The surface impedance of the wall is inductive if $0 < d_{eff.} < \lambda_s/4$ and $\lambda_s/2 < d_{eff.} < 3\lambda_s/4$, and capacitive if $\lambda_s/4 < d_{eff.} < \lambda_s/2$. On the basis of the design rules, the slots are designed to approximate a metallic waveguide by setting the depth at a half of the wavelength, i.e., $d_{eff} = \lambda_s/2 \sim 0.2$ mm. According to (1), surface reactance becomes simply zero and the impedance of inner wall becomes resistive. By this design, the slot depth also satisfies the condition for impedance matching between the feeding metallic waveguide and LTCC hollow waveguide for measurement purposes.

The transmission characteristics of the waveguide are determined by a, s, t, and d. It should be noted that d_{eff} is affected by a and s. Using commercial finite element method (FEM) simulation software, we numerically analyzed the influence of slot depth on the transmission characteristics of the waveguide. In the model, both sides of the 2-mm LTCC waveguide, whose size is 0.8×0.4 mm^2, are connected to a metallic WR3.4 waveguide. The inner wall of the waveguide is corrugated with dielectric loaded on both the E and H planes. We equally vary the slot depth on both the E and H plane in the simulation. Fig. 3 shows the simulated $|S_{11}|$ of the LTCC hollow waveguide for different slot depths. The simulation results show that the return loss (S_{11}) of the waveguide is more than 15dB above 254 GHz for $d \geq 0.20$ mm. As the slot depth increases, the center frequency shifts to lower frequency. And the return loss is minimized in the 300-GHz band for $d = 0.24$ mm. Fig. 4 shows the simulated $|S_{21}|$ of the LTCC hollow waveguide for different slot depths. As the slot depth increases, the cut-off frequency shifts to lower frequency. The cut-off characteristic is well described by an equivalent circuit model analysis, in which corrugation along the waveguide is modeled as a series of capacitances and shunt inductances [19]. Despite the dielectric loss of LTCC, insertion loss (S_{21}) is less than 0.3 dB/mm at 300 GHz for $d = 0.20$ mm and less than 2 dB from 266 to 350 GHz. The insertion loss increases because of

This article has been accepted for publication in a future issue of this journal, but has not been fully edited. Content may change prior to final publication. Citation information: DOI 10.1109/TAP.2014.2350520, IEEE Transactions on Antennas and Propagation

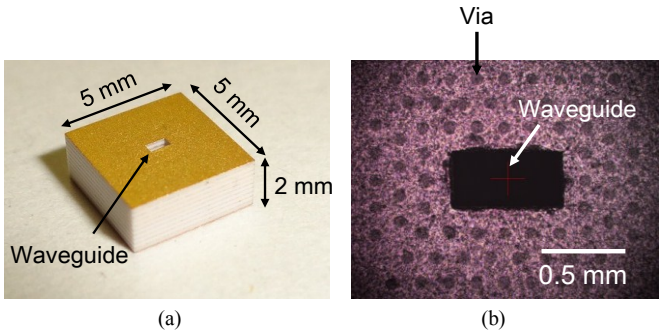

Fig. 5. Photograph of the fabricated LTCC hollow waveguide. (a) Overall view of LTCC substrate; (b) microphotograph of the waveguide.

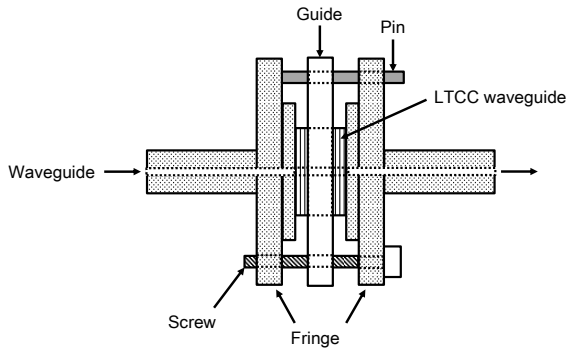

Fig. 6. Schematic view of the measurement setup.

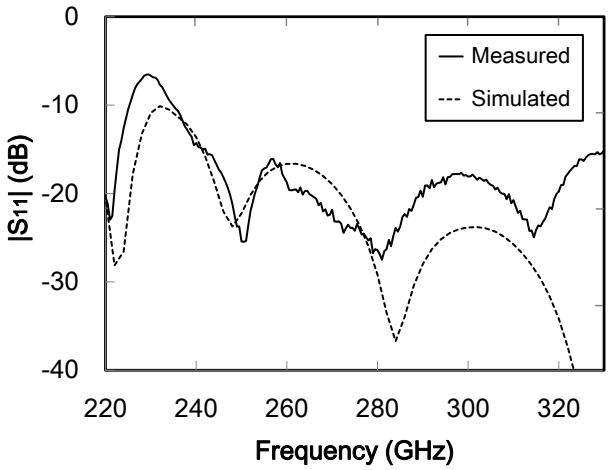

Fig. 7. Measured and simulated $|S_{11}|$ of the LTCC waveguide for slot depth d = 0.20 mm.

inductive current above 300 GHz for d = 0.24 mm.

To verify the numerical analysis, a 2-mm LTCC waveguide was fabricated for d = 0.20 mm by stacking 20 layers. A photograph of the test substrate is shown in Fig. 5. The silver patterns on the top and bottom layers are metalized by Ni/Au electroplating. The waveguide size was set the same as that of the simulation model. The LTCC waveguide was measured with a vector network analyzer (Agilent E8362B) and WR3 extenders (Virginia Diodes). To feed the LTCC waveguide, we sandwiched the substrate with a metal guide between the flanges as shown in Fig. 6. The accuracy of the alignment is

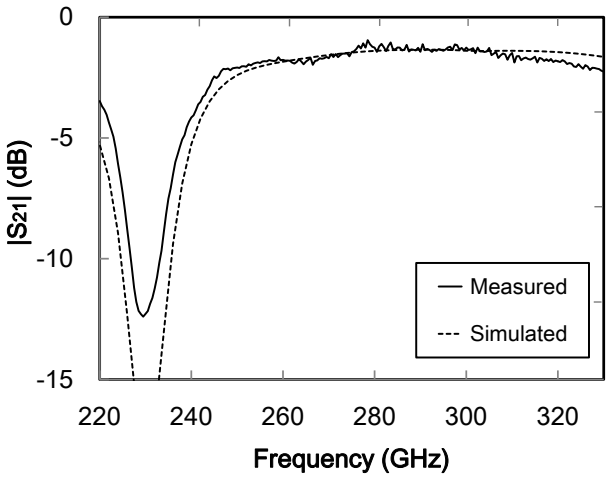

Fig. 8. Measured and simulated $|S_{21}|$ of the LTCC waveguide for slot depth d = 0.20 mm.

limited by the milling precision of the guide and the fabrication tolerance of the LTCC substrate. Considering theses errors, the accuracy of the alignment is estimated to be less than 50 μm. Figs. 7 and 8 show the measured S-parameters (insertion and return loss). The measured insertion loss is less than 0.6 dB/mm and the 15 dB-bandwidth ranges from 242 to 330 GHz. The loss due to leakage of electromagnetic waves and the inductive surface doesn't become prominent around 300 GHz. The LTCC waveguide exhibits low-loss transmission and well-matches the impedance of metallic waveguide in the 300-GHz band. The measurement shows good agreement with the simulation. At lower frequency below 250 GHz, the dip at 230 GHz in the measurement is blunter than in the simulation. The frequency of the dip depends on the slot depth. Thus, we think the fabrication variation in the slot depth caused the bluntness. Above 300 GHz, the insertion loss is relatively high compared to the simulation results because of the error in the conductivity of silver and loss tangent of the LTCC and because of misalignment between the LTCC waveguide and metal waveguides.

C. Stepped Horn Antenna with Corrugation

Horn antennas are created by flaring the dimension of a rectangular waveguide along both the *E* plane and the *H* plane. The flare of the horn antenna is formed by the stepped cavity surrounded by the via fence and metal layers. The horn antenna is considered to have a structure equivalent to that of a conventional corrugated horn antenna like the LTCC waveguide does. In the common design, the slot depths of corrugated horn antennas are gradually tapered from $\lambda_0/2$ to $\lambda_0/4$ starting at the horn throat to smoothly convert TE_{10} into HE_{10} [20]. However, the design rules for our SIW horn antennas don't follow the same principles as for conventional corrugated horns because of fabrication limitations concerning the slot depth as described above. Thus, keeping the slot depth at the same depth as the feeding throat, we approximate a metal pyramidal horn antenna.

This article has been accepted for publication in a future issue of this journal, but has not been fully edited. Content may change prior to final publication. Citation information: DOI 10.1109/TAP.2014.2350520, IEEE Transactions on Antennas and Propagation

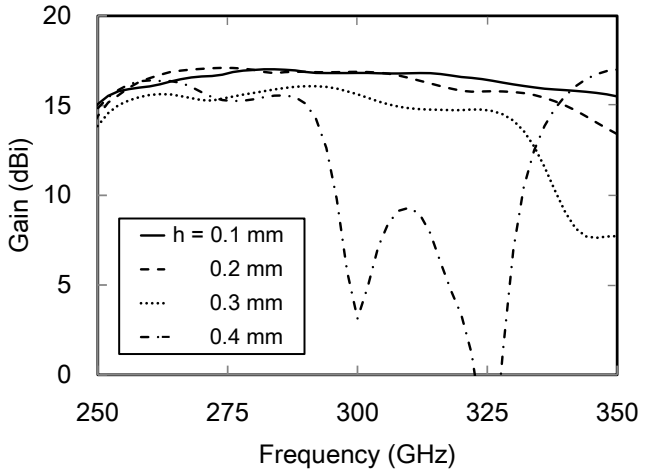

Fig. 9. Simulated antenna gain of the LTCC horn antenna for different step sizes (d = 0.20 mm).

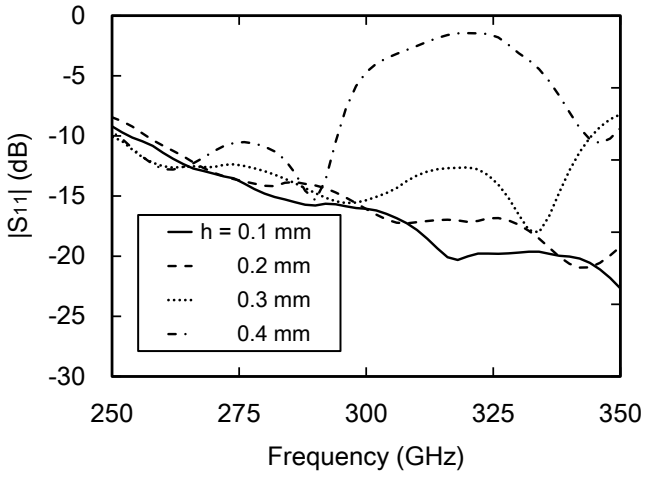

Fig. 10. Simulated $|S_{11}|$ of the LTCC horn antenna for different step sizes (d = 0.20 mm).

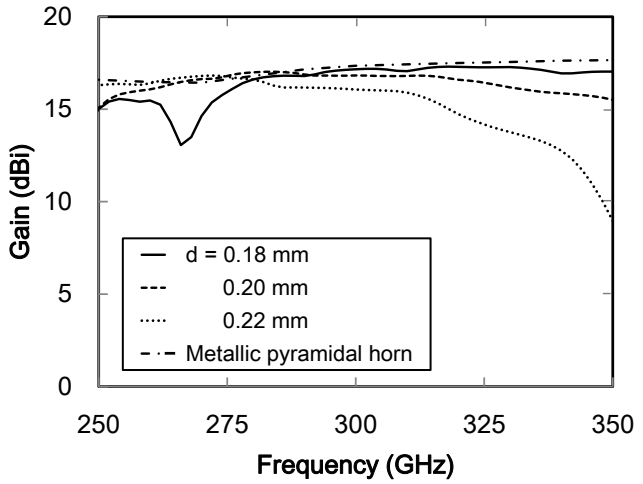

Fig. 11. Simulated antenna gain of the LTCC horn antenna for different slot depths and of a metallic horn with the same horn length and aperture size for comparison.

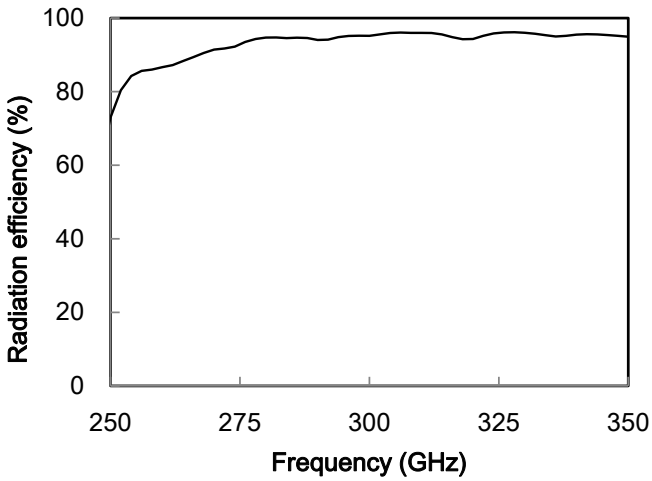

Fig. 12. Simulated radiation efficiency of the LTCC horn antenna.

The horn length, effective horn flare angle and stepped profile are the design parameters. The horn length is simply determined by the total thickness of the LTCC and metal layers. As the total thickness is limited to 3.0 mm, we used 24 LTCC layers for the flare section and three LTCC layers for the horn throat. Next, we set the effective flare angle to 26° to maximize the antenna gain with respect to the aperture size of the optimum horn. In the step-profile, the step height is determined by the number of 0.1-mm-thick LTCC layers used in a step. The stepped profile requires a different cavity and via drilling process in each layer, so that reducing number of steps and these processes makes the SIW horn antenna easy to fabricate. However, larger step discontinuities cause phase error effects and a reduction of the antenna aperture efficiency. From the standpoint of impedance variation along the flare, a step-profiled diagonal horn antenna has been analyzed by using a numerical approach with a scattering matrix [21]. We performed FEM simulation of the characteristics of an antenna whose step profile has different step heights but with the same effective flare angle and horn length. The gain and simulated $|S_{11}|$ for different step heights are shown in Figs. 9 and 10. With a good approximation to the gain characteristics of the smooth-profiled horn, we found that the step discontinuities should be 0.1 mm or 0.2 mm. As can be seen in the Fig. 10, the largest step height (h = 0.4 mm) causes strong return loss at 300-GHz band; however, the return loss decreases by decreasing the step size. Our previous study showed that antenna gain of an LTCC horn antenna with 0.3-mm step height is degraded by the manufacturing tolerances in step formation [13]. Taking into account the previous results, we set the step height at the minimum value of 0.1 mm (single layer of 0.1-mm thickness LTCC) for better tolerance to the manufacturing variation in step size. Consequently, the step width is set as 0.05 mm for a 26°flare angle.

Finally, we numerically analyzed the influence of slot depth on the antenna characteristics of the horn antenna. Fig. 11 shows the frequency dependence of the simulated gain of the horn antenna for different slot depths. In the numerical model, the LTCC horn antenna is fed by a metallic WR3.4 standard waveguide. The simulation shows that the horn antenna

This article has been accepted for publication in a future issue of this journal, but has not been fully edited. Content may change prior to final publication. Citation information: DOI 10.1109/TAP.2014.2350520, IEEE Transactions on Antennas and Propagation

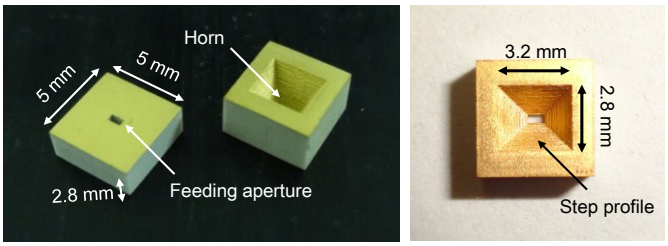

(a) (b)

Fig. 13. Photograph of the prototype of the LTCC horn antenna.(a) Overall view of LTCC substrate; (b) top view.

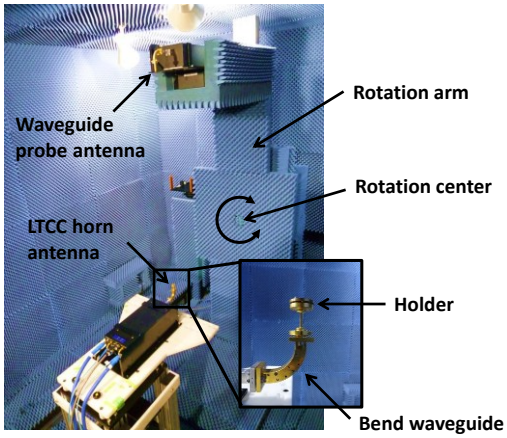

Fig. 14. Photograph of the measurement setup.

exhibits the gain of 17 dBi at 300GHz and more than 15-dBi gain from 250 to 350 GHz for d = 0.20 mm. The antenna gain at 300 GHz is comparable to that of a smooth-profiled metallic pyramidal horn with the same dimension. For the inner wall of the metallic horn, the conductivity of gold is 4.1 ×10^7S/m. The stepped profile doesn't cause phase error effects or internal reflection and it succeeds in approximation of metallic horns. The horn antenna for d = 0.18 mm exhibits a dip in the gain at 270 GHz due to the corrugation at inner wall, which is also observed in the measured insertion loss of the LTCC waveguide. The horn antenna for d = 0.22 mm exhibits a decrease in gain above 275 GHz.

Radiation efficiency of the horn antenna was simulated in the similar manner in [7]. Fig. 12 shows the radiation efficiency of the horn antenna for d = 0.20 mm. The simulation shows that the horn antenna exhibits radiation efficiency of more than 80 %from 252 to 350 GHz for d = 0.20 mm. Even though the dielectric loss of LTCC is relatively high, high efficiency is achieved thanks to the hollow structure.

III. Measurement

The prototype of the LTCC horn antenna for d = 0.20 mm was fabricated by stacking 27 layers using the LTCC multi-layer process. A photograph of the prototype is shown in Fig. 13. The overall size is 5×5×2.8 mm^3. The width and height of the steps along the flare are 0.05 and 0.1 mm, respectively. The size of the horn aperture is 3.2 ×2.8 mm^2. On the bottom

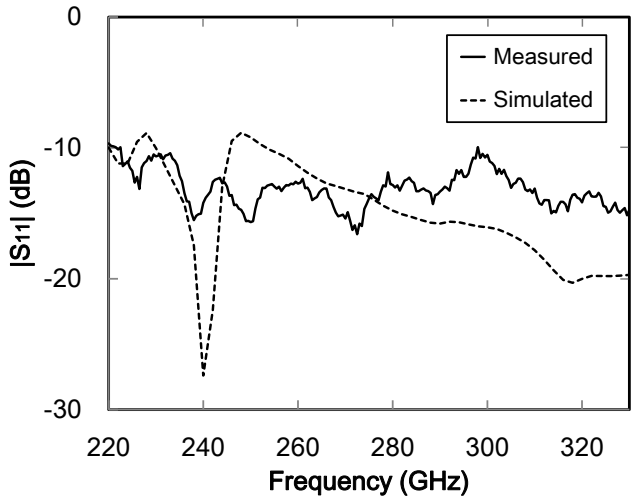

Fig. 15. Measured and simulated $|S_{11}|$ of the horn antenna.

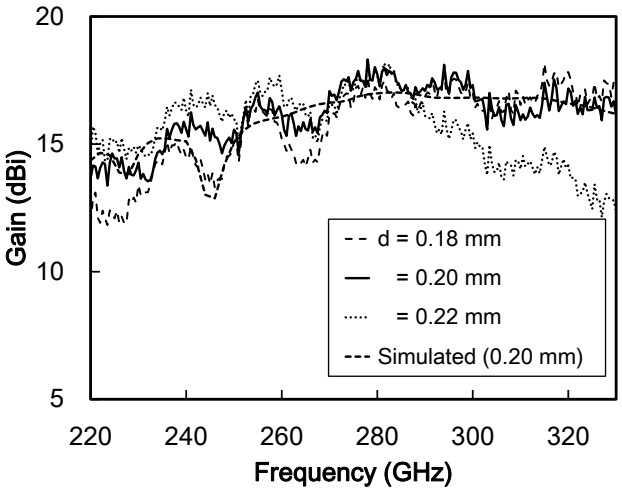

Fig. 16. Measured and simulated antenna gain of the horn antenna.

side of the prototype, the size of the feeding waveguide aperture is 0.8×0.4 mm^2.

The characteristics of the LTCC horn antenna were measured in an anechoic chamber. Fig. 14 shows a photograph of the measurement setup. The antenna was mounted on the flange of a metallic WR3.4 standard waveguide for feeding. The alignment between the feed waveguide aperture and the antenna's input port was made by using the metal holder with a guide. At the opposite side of the antenna, a 6-dBi waveguide probe antenna was attached to the 180-degree rotation arm to measure the radiation pattern. The distance between the antennas was 1 m, which is long enough for far-field approximation. The alignment between the two antennas was adjusted by using a line laser level.

Fig. 15 shows the simulated and measured $|S_{11}|$ of the horn antenna. The return loss is more than 10 dB from 230 to 330 GHz. The difference between the simulation and experiment is mainly due to the misalignment between the LTCC waveguide and metal waveguides. Fig. 16 shows the measured antenna gain for different slot depths and the simulated gain for d = 0.20 mm. The antenna gain was calculated using a 25-dBi standard pyramidal horn antenna whose gain was calibrated with the

This article has been accepted for publication in a future issue of this journal, but has not been fully edited. Content may change prior to final publication. Citation information: DOI 10.1109/TAP.2014.2350520, IEEE Transactions on Antennas and Propagation

TABLE II
COMPARISON TO OTHER LTCC SIW ANTENNAS AND A METALLIC PYRAMIDAL HORN

Frequency (GHz)	Antenna Topology	Size (mm^3)	Impedance bandwidth (GHz)	Maximum gain (dBi)	3-dB gain bandwidth (GHz)	Simulated radiation efficiency (%)	Fabrication complexity	Reference
300	Step-profiled Corrugated horn	2.8 ×3.2 ×2.7	100 (−10dB)	18	72	90	Required cavity 27 layers	This study
300	Smooth-profiled metallic horn	2.8 ×3.2 ×2.7	110 (-15dB)	18	110	~100	Required milling	simulation
140	Slot antenna array	23 × 20 ×0.76	28.6 (−10dB)	16.3	22	70	No cavity 6 layers	[6]
140	Slot antenna array	10.8 × 15.1×1.1	21 (−10dB)	21.3	16.8	46.6	No cavity 11 layers	[7]
270	Slot antenna array	$14^2\pi \times 0.49$	20.9 (−10dB)	27.6	9.8	73	No cavity 5 layers	[8]
270	Fresnel zone plate lens	$7.3^2\pi \times 1.87$	10 (−8dB)	20.8	9.1	38	No cavity 20 layers	[9]

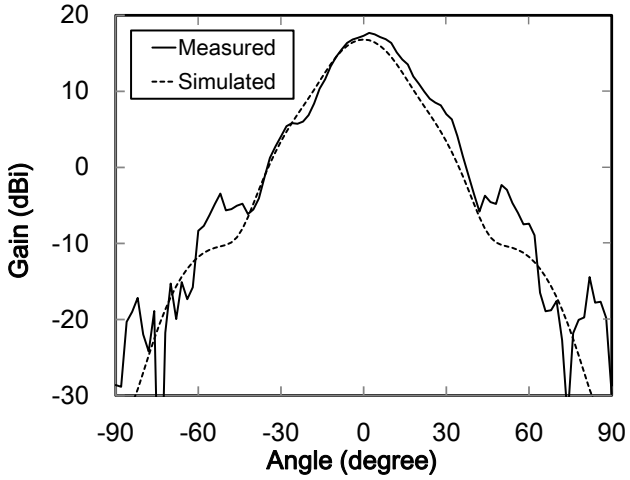

Fig. 17. Measured and simulated *E* plane radiation patterns at 300 GHz.

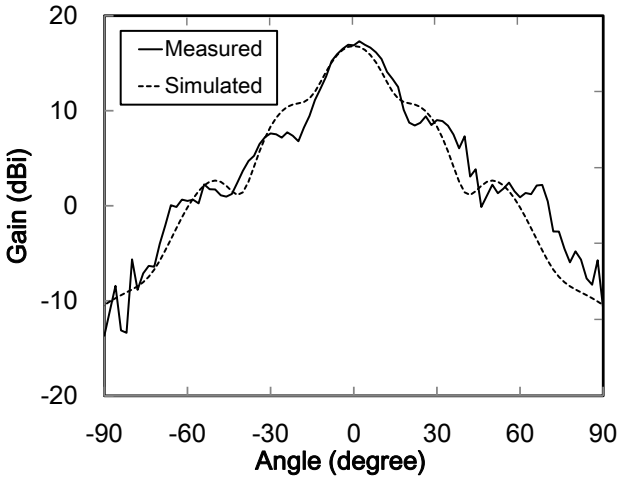

Fig. 18. Measured and simulated *H* plane radiation patterns at 300 GHz.

three-antenna method. For d = 0.20 mm, the antenna gain is more than 15 dBi from 248 to 320 GHz, and its peak value is 18 dBi. The antenna gain for d = 0.22 mm decreases above 280 GHz as predicted in the simulation in Fig. 11. For d = 0.20 mm, the measurement shows good agreement with the simulation. The discrepancy between them could be due to variation of the step size or slot depth. Fabrication tolerances are not considered to cause a significant degradation in antenna bandwidth and gain. The dip in the gain at 240 GHz in the simulation for d = 0.20 mm is also observed in the measurement of the LTCC waveguide as shown in Fig. 8. The dips mainly originate from the corrugation at the feeding waveguide of the antenna. Figs. 17 and 18 show the simulated and measured radiation patterns at 300 GHz in both the *E* and *H* planes. The 3-dB beamwidths of the *E* and *H* planes are 24 and 22 °, respectively. The measurement shows good agreement with the simulation. The slight asymmetry in the patterns originates from bending of the substrate and asymmetrical variation in the step profile.

IV. CONCLUSIONS

A 300-GHz horn antenna aiming at integration on LTCC packages is presented. Experimental results show the transmission loss of the hollow LTCC waveguide is low enough to be applicable to the 300-GHz antenna. We find the utilization of the hollow waveguide is essential for low-loss transmission in high-dielectric loss material. On the basis of the numerical analysis, we set the slot depth of corrugation to minimize the return loss and maximize the antenna gain in the 300-GHz band. The prototype of a LTCC horn antenna has a peak value of 18-dBi antenna gain and 100-GHz bandwidth with more than 10-dB return loss. The vertically formed hollow structure can reduce dielectric loss of LTCC an]d enhance antenna efficiency, and it can be fabricated without any special fabrication process. The experimental results have good agreement with simulations and confirm that optimizing the slot depth of the corrugation and the step height is the key to achieve high gain and wide bandwidth.

Table II summarizes the performance of the presented 300-GHz LTCC horn antenna with a smooth-profiled metallic horn and that of other reported SIW antennas above 100 GHz. Although the antenna gain at 300 GHz is comparable to that of the smooth-profiled horn with the same dimensions, the gain isn't the highest among the other LTCC antennas. Note, however, that the aperture areas with higher gain are larger than that of the proposed antenna. Although the gain of the proposed antenna could be increased by increasing the number of layers, cavity formation with a large number of layers would increase

This article has been accepted for publication in a future issue of this journal, but has not been fully edited. Content may change prior to final publication. Citation information: DOI 10.1109/TAP.2014.2350520, IEEE Transactions on Antennas and Propagation

the fabrication complexity. The impedance bandwidth, 3-dB gain bandwidth, and radiation efficiency are the best among antennas in this frequency range. The wide bandwidth of the proposed antenna is the main feature for applying the antenna to high data-rate communications. Thanks to the hollow structure, the efficiency is highest among the other LTCC antennas. The proposed LTCC horn antenna is compact in aperture size and easy to integrate in low-cost LTCC transceiver modules.

It is also worth mentioning that the utilization of corrugation enables the horn antenna to exhibit better *E*/*H* symmetry of the radiation patterns and a better Gaussian profile, which make the modules more suitable for use in combination with a lens and mirrors for quasi-optical beam scanning techniques.

ACKNOWLEDGMENT

The authors thank Katsumi Fujii and Toshihide Tosaka from the National Institute of Information and Communications Technology for the measurement of antenna gain.

REFERENCES

[1] H.-J. Song, and T. Nagatsuma, "Present and Future of Terahertz Communications", *IEEE Trans. on Terahertz Science and Technology*, Vol. 1, No. 12, pp. 256–263, Sept. 2011.

[2] T. Schnider, A. Wiatrek, S. Preuβler, M. Grigat, and R-P Braun, "Link Budget Analysis for Terahertz Fixed Wireless Links", *IEEE Trans. on Terahertz Science and Technology*, Vol. 2, No. 2, pp. 250–256, Mar. 2012.

[3] H.-J. Song, K. Ajito, Y. Muramoto, A. Wakatsuki, T. Nagatsuma, and N. Kukutsu, "24 Gbit/s data transmission in 300 GHz band for future terahertz communications", *Electron. Lett.*, Vol. 48, No. 15, pp. 953–954, Jul. 2012.

[4] Y. P. Zhang, M. Sun, K. M. Chua, L. L. Wai, and D. Liu, "Antenna-in-Package Design for Wirebond Interconnection to Highly Integrated 60-GHz Radios", *IEEE Trans. on Antennas and Propagation*, Vol. 57, No. 10, pp. 2842–2852, Oct. 2009.

[5] Junfeng Xu, ZhiNing Chen, Xianming Qing, and Wei Hong, "140-GHz Planar Broadband LTCC SIW Slot Antenna Array," *IEEE Trans. on Antenna and Propagation*, vol. 60, no. 6, pp. 3025–3028, 2012.

[6] Junfeng Xu, ZhiNing Chen, Xianming Qing, and Wei Hong, "140-GHz TE20-Mode Dielectric-Loaded SIW Slot Antenna Array in LTCC," *IEEE Trans. on Antenna and Propagation*, vol. 61, no. 4, pp. 1784–1793, 2013.

[7] JunfengXu, ZhiNing Chen, and Xianming Qing,"270-GHz LTCC-Integrated Strip-Loaded Linearly Polarized Radial Line Slot Array Antenna",*IEEE Trans. on Antennas and Propagation*, Vol. 61, No. 4, April 2013, pp. 1794–1801.

[8] JunfengXu, ZhiNing Chen, and Xianming Qing,"270-GHz LTCC-Integrated High Gain Cavity-Backed Fresnel Zone Plate Lens Antenna", *IEEE Trans. on Antennas and Propagation*, Vol. 61, No. 4, April 2013, pp. 1679–1687.

[9] S. B. Yeap, X. Qing, M. Sun, and Z. N. Chen, "140GHz 2×2 SIW horn array on LTCC", *IEEE Asia-Pacific Conference on Antennas and Propagation,*Augst. 2012, pp. 279–280.

[10] H. Wang, D.-G. Fang, B. Zhang, and W.-Q. Che, "Dielectric loaded substrate integrated waveguide (SIW) H-plane horn antennas," *IEEE Trans. Antennas and Propagation*, vol. 58, no. 3, pp. 640–647, Mar. 2010.

[11] M. Esquius-Morote, B. Fuchs, J-F Zurcher, J. R. Mosig, "Novel Thin and Compact H-Plane SIW Horn Antenna", *IEEE Trans. on Antennas and Propagation*, Vol. 61, No. 6, June 2013, pp. 2911–2920.

[12] Y. She, J. Hirokawa, M. Ando, D Hanatani, M. Fujimoto, "LTCC Partially-Filled Post-Wall Rectangular-Waveguide Slot Array Antenna in the Millimeter-Wave Band", *IEICE TRANS. ELECTRON.*, Vol. E95-C, No.10, Oct. 2012, pp. 1635–1642.

[13] T. Tajima, H.-J. Song, K. Ajito, M. Yaita, and N. Kukutsu, "300-GHz LTCC Horn Antennas Based on Antenna-in-Package Technology," *the 43rd European Microwave Conference*, Sept. 2013, pp. 231–234.

[14] G. H. Bryant, "Propagation in corrugated waveguides", *PROC. IEE*, Vol. 116, No. 2, Feb. 1969, pp. 203–213.

[15] C. A. Mentzer and L. Peters," Properties of Cutoff Corrugated Surfaces for Corrugated Horn Design",*IEEE Trans. on Antennas and Propagation*, Vol. AP-22, No. 2, Mar.1974, pp. 191–196.

[16] J. Esteban, and J. M. Rebollar, "Characterization of Corrugated Waveguides by Modal Analysis", *IEEE Trans. on Microwave Theory and Techniques*, Vol. 39, No. 6, pp. 937–943, June, 1991.

[17] R. Baldwin and P. A. McInnes, "Corrugated rectangular horns for use as microwave feeds", *Proc. Inst. Elec. Eng.,* vol. 122, pp. 465–469, May 1975.

[18] C. A. Balanis, "Horn Antennas"in *Antenna Theory*, 3rd ed.,New Jersey: John Wiley& Sons, 2005, pp. 785–791.

[19] I. A. Eshrah, A. A. Kishk, A. B. Yakovlev, and A. W. Glisson, "Rectangular Waveguide With Dielectric-Filled Corrugations Supporting Backward Waves", *IEEE Trans. on Microwave Theory and Techniques*, Vol. 53, No. 11, pp. 3298–3304, Nov.2005.

[20] C. Witebsky, G. F. Smoot, Steven Levin, and M. Bensadoun,"A Large L-band Rectangular Corrugated Horn", *IEEE Trans. on Antennas and Propagation*, Vol. AP-35, No. 11, Nov.1987, pp. 1310–1313.

[21] G. V. Eleftheriades, and G. M. Rebeiz, "High-Gain Step-Profiled Integrated Diagonal Horn-Antennas", *IEEE Trans. on Microwave Theory and Techniques*, Vol. 40, No. 5, pp. 801–805, May1992.

Takuro Tajima(S'03–M'04)received the B.S. and M.E. degrees from the University of Tokyo, Tokyo, Japan, in 2002 and 2004, respectively.

In 2004, he joined Nippon Telegraph and Telephone Corporation (NTT), Telecommunication Energy Laboratories, Kanagawa, Japan, where he was engaged in the research and development of measurement technologies for photo-acoustic non-invasive biosensors. Since 2012, he has been engaged in the research and development of sub-terahertz antennas and packages. He is currently a Senior Research Engineer with NTT Device Technology Laboratories, Kanagawa, Japan. His current research involves millimeter-wave and sub-terahertz-wave radio transmission.

Mr. Tajima is a member of the Institute of Electronics, Information and Communication Engineers (IEICE), Japan.

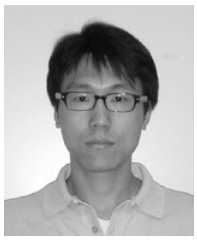

Ho-Jin Song (S'02–M'06-SM'13) received the B.S. degree in electronics engineering from Kyungpook National University, Daegu, Korea, in 1999, and the M.S. and Ph.D. degrees in information and communications engineering from Gwangju Institute of Science and Technology, Gwangju, Korea, in 2001, and 2005, respectively.

From 2005 to 2006, he was involved with the Center for Hybrid Optical Access Networks, Gwangju Institute of Science and Technology, Gwangju, Korea, as a Research Professor, where he was engaged in research on millimeter-wave communications systems utilizing radio-over-fiber technologies. Since joining Microsystem Integration Laboratories, Nippon Telegraph and Telephone Corporation (NTT),Atsugi, Kanagawa, Japan, in 2006, he has been working on the development of millimeter-wave and sub-terahertz wave systems for communications, sensing, imaging, and measurement applications using photonic technologies and high-speed electronics.

Dr. Song is a member of the Institute of Electronics, Information and Communication Engineers (IEICE), Japan.

Katsuhiro Ajito(A'11–M'12) received the

This article has been accepted for publication in a future issue of this journal, but has not been fully edited. Content may change prior to final publication. Citation information: DOI 10.1109/TAP.2014.2350520, IEEE Transactions on Antennas and Propagation

Ph.D.degree in applied chemistry from the University of Tokyo, Tokyo, Japan, in 1995.

He is a Senior Research Scientist with the Smart Devices Laboratory, NTT Microsystem Integration Laboratories, and a Distinguished Technical Member of the NTT Science and Core Technology Laboratory Group, Atsugi, Japan. He joined NTT Basic Research Laboratories in 1995. From 1995 to 2007, he studied glutamate in single synapses using Raman spectroscopy and laser tweezers. His current research interests include nano- and biochemistry studied by terahertz spectroscopy and imaging techniques.

Dr.Ajito is a member of the Spectroscopical Society of Japan (SSJ), Japan Society of Applied Physics (JSAP), the Chemical Society of Japan, and the American Chemical Society. He was the recipient of the Young Scientist Award for the Presentation of an Excellent Paper from the JSAP in 1999. He has been the Executive Director and the Chair of the Terahertz Spectroscopy Division of the SSJ since 2005, the Secretary of the Terahertz Interest Group in IEEE 802.15Working Group for wireless personal area networks since 2011, and the Chair of the Micro/Nano Electromechanical Systems and Bio/Medical Analyses Area of the International Conference on Solid State Devices and Materials in JSAP since2012.

Makoto Yaita received the B.S. and M.E. degrees from Waseda University, Tokyo, Japan, in 1988 and1990, respectively.

In 1990, he joined Nippon Telegraph and Telephone Corporation (NTT), LSI Laboratories, Kanagawa, Japan, where he was engaged in the research and development of measurement technologies for high-speed devices and ultrafast-optical signals. From 1999 to 2008, he was engaged in the development of the digital television relay network for NTT Communications. He is currently a Senior Research Engineer and Supervisor with NTT Device Technology Laboratories, Kanagawa, Japan. His current research involves millimeter-wave and sub-terahertz-wave radio transmission.

Naoya Kukutsu(M'93) received the B.E., M.E., and D.E. degrees in electrical engineering from Hokkaido University, Sapporo, Japan, in 1986, 1988 and 1991, respectively. His D.E. dissertation described research on a time-domain electromagnetic wave numerical analysis method. In 1991, he joined the Nippon Telegraph and Telephone Corporation (NTT), Applied Electronics Laboratories, Musashino, Japan. From 2008 to 2013, he was engaged in research on millimeter-wave and terahertz-wave radio transmission and imaging systems as a Leader of a research group with NTT Microsystem Integration Laboratories, Atsugi, Japan. He is currently a Senior Research Engineer, Supervisor with Wave Engineering Laboratories in Advanced Telecommunications Research Institute International, Kyoto, Japan, as the head [Comment: There can only be one head of a department; therefore, 'the head' is correct.] of the research department for developing new applications using electromagnetic waves.

Dr. Kukutsu is a senior member of the Institute of Electronics, Information, and Communication Engineers of Japan and a member of the IEEE Microwave Theory and Techniques Society (MTT-S) and Communication Society.